

SUPPLEMENTARY DISCUSSIONS TO MANUSCRIPT:
Ultrahigh Strength and Shear-Assisted Decohesion of Sliding Silver Nanocontacts Studied
in situ

Supplementary Discussion 1 (the results to obtain the values of spring constant)

We obtained the stiffness of the beam through analytical, numerical, and experimental means. The results of these analyses agree to within 1.4% giving confidence in the result.

Table S.1 | The experimental values of the spring constant were compared with analytical and numerical solutions.

	Analytical value	Numerical value	Experimental value
k_x	3.1	3.09	3.1
k_y	30	29.6	30

The analytical value of the stiffness k is calculated by Eq.6.

$$k = \frac{Ew^3t}{4l^3} \quad (6)$$

The stiffness k_x for measuring the friction force F was calculated by Eq.6 where the Young's modulus E is 169.7 GPa, the width of the beam w , the length of the beam l , and the thickness of the beam t were measured by SEM as 6.5, 80, and 670 μm , respective

$$k_x = 3.1 \text{ [N/m]}$$

The stiffness k_y for measuring the normal force N was calculated by Eq.6. where the Young's modulus E 169.7 GPa, the width of the beam w , the length of the beam l , and the thickness of the beam t were measured by SEM as 17.5, 80, and 850 μm respective.

$$k_y = 30 \text{ [N/m]}$$

The numerical method calculates the stiffness k_x for measuring the friction force F . In order to estimate the stiffness of the beam corresponding to the first normal mode, Finite Element analysis was performed. In this analysis, a point load of $1\mu\text{N}$ was applied to the end of the cantilever, while the other side of the beam was held fixed. This resulted in a tip displacement of $0.323\ \mu\text{m}$, which translates to a beam stiffness of $3.09\ \text{N/m}$.

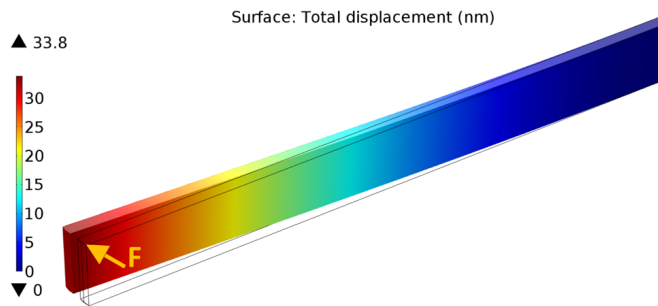


Figure S16 | A finite element analysis calculated the displacement by the applied force (the stiffness k_x). The right edge of the beam was fixed, and the left side was free. The force was applied at the very end of the left beam. The values of the width of the beam, the length of the beam and thickness of the beam were matched to the SEM measurements.

The numerical method calculates the stiffness k_y for measuring the load. The stiffness of the beam k_y was derived through a similar procedure to that used to calculate the stiffness in the x direction. A point load of $1\mu\text{N}$ was applied to the end of the cantilever, while the other side of the beam was held fixed. This resulted in a tip displacement of $0.0338\ \mu\text{m}$, which translates to a stiffness of the beam of $29.6\ \text{N/m}$.

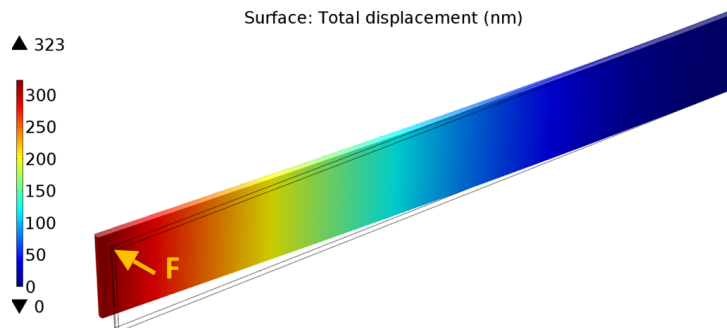


Figure S17 | A FEM analysis calculated the displacement by the applied force (the stiffness k_y).

The beam stiffnesses were obtained by measuring the resonant frequency. The resonant frequency and mass of the beam can be used to derive the stiffness of the beam:

$$f = \frac{1}{2\pi} \sqrt{\frac{k}{M'}} \quad (7)$$

where f is the resonant frequency, k is the stiffness of the beam and M' is the effective mass of the beam.

The effective mass of the first normal mode M' corresponds to 23% of the gravitational M .

$$M' = 0.23M \quad (8)$$

The gravitational mass M was calculated from the density ρ [kg/m³], the width of the beam w , the length of the beam l and the thickness of the beam t .

$$M = \rho w l t \quad (9)$$

Then, Eq.7~9 gives,

$$f = \frac{1}{2\pi} \sqrt{\frac{k}{0.23\rho w l t}}$$

$$k = 1.04\pi^2 f^2 \rho w l t \quad (10)$$

In order to measure the stiffness of the beam, we applied an alternating input voltage. This voltage induced current flow through the beam due to the change of the capacitance between the beam and the actuator. We detected this current using a lock-in-amplifier. For a given voltage maximum amplitude, the largest vibrational displacement is achieved at the beam's resonant frequency. When the beam moves, the gap between the beam and the electrostatic actuator becomes narrow inducing additional current flow, so the current is maximized at the resonant frequency.

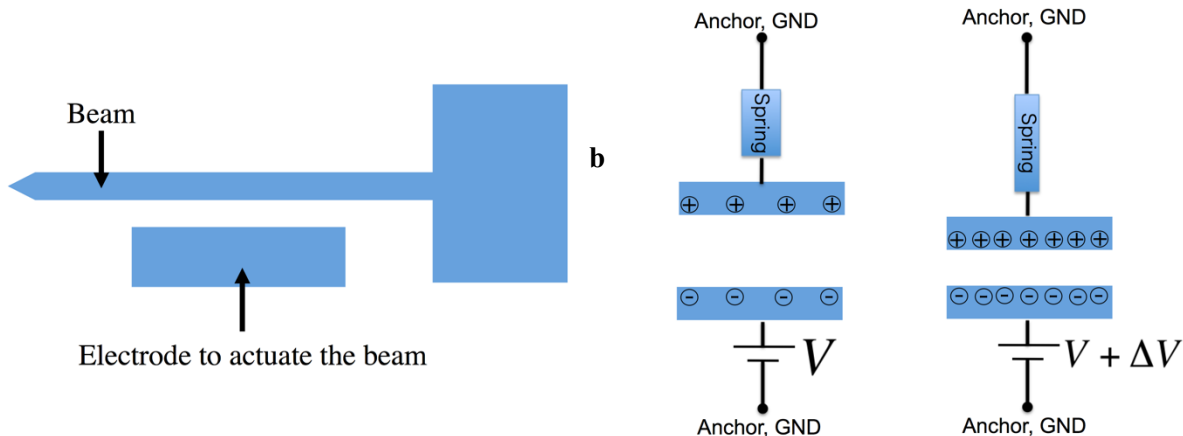


Figure S18 | The fundamentals of the electrostatic actuator and inducing vibrations. **a** the electrostatic actuator was integrated alongside the long beam. The beam was treated as a spring and the beam/actuator were treated as a capacitor, as depicted in **b** and **c**. **b** the input voltage generates electrical charges between capacitors that applies an actuation force between the beam and the actuator. **c** an increase in the input voltage further attracts the beam. A sinusoidal voltage generates beam vibrations.

An electrostatic actuator has a spring effect, which makes the beam appear softer than we expect. When the beam is actuated, the gap between the beam and actuator becomes smaller, thereby increasing the magnitude of the electrostatic attractive force. This causes the beam to deflect more than otherwise expected at higher input voltages. This phenomenon is known as the “spring effect”. In order to measure the actual stiffness of the beam independent of the spring effect, a bias voltage between the beam and the electrostatic actuator was applied. We detected the resonant frequency for each bias voltage and then obtained the mechanical stiffness while eliminating the effect of the applied input voltage.

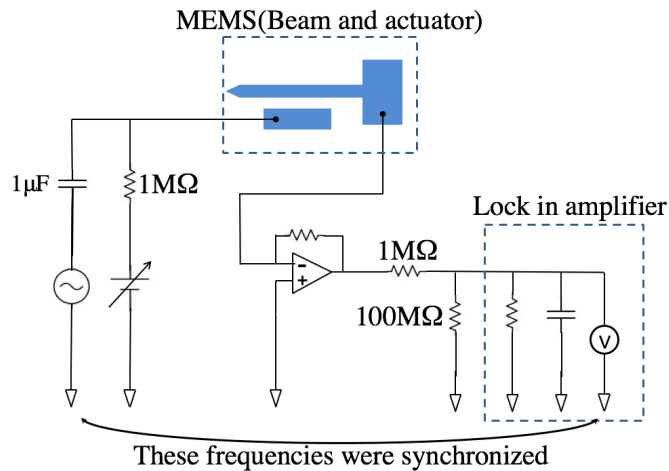


Figure S19 | A function generator and lock in amplifier allow measurement of the beam resonant frequency. The input voltage was applied from the electrostatic actuator to the beam. The current flows to the beam. The current was magnified and monitored by lock-in-amplifier.

An alternating input voltage and a bias voltage of 60 V were applied at the electro static actuator. We detected the current and found that the resonant frequency was 20.087 kHz. We changed the bias voltage and measured the resonant frequency for each bias voltage as shown below.

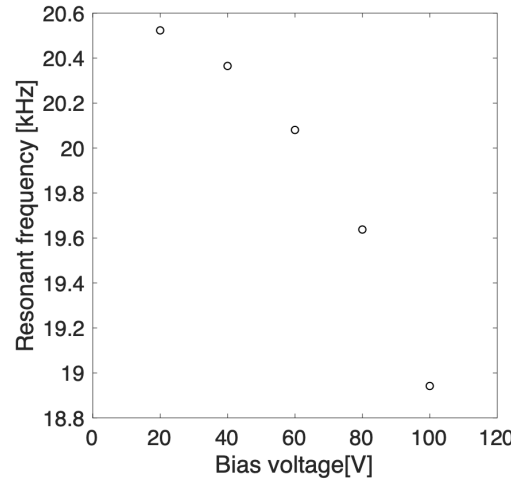


Figure S20 | The resonant frequencies of k_x beam were measured for each bias voltage. The resonant frequency at the bias voltage as 0 V was utilized to calculate the stiffness.

The resonant frequency when the bias voltage V_{bias} was zero, corresponds to the stiffness that does not include the spring effect. According to the relationship between the bias voltage V_{bias} and the resonant frequency f , we obtained $f = -0.2199V_{bias}^2 + 6.9394V_{bias} + 20461$. We found that the resonant frequency for detecting the force was 20.46[kHz]. The equation (4) and the value of resonant frequency give the value of the stiffness. Therefore, we found that the stiffness k_x was 3.1[N/m]. The maximum of this function should be at $V=0$, however the maximum is at $V \sim 16V$ so at $V=0$ it is lower than the maximum of ~ 20.52 KHz. This is a very small error though, only 0.2% which is fairly equal to the precision of the experiments. Furthermore fixing it here won't change the 3.1N/m number that propagates into all your other calculations.

$$\begin{aligned}
 k_x &= 9.08 \times (20461)^2 \times 2329[\text{Kg/m}^3] \times (6.5 \times 10^{-6}) \times (670 \times 10^{-6}) \times (80 \times 10^{-6}) \\
 &= 3.084[\text{N/m}]
 \end{aligned}$$

$$=3.1 \text{ [N/m]}$$

The stiffness of the beam k_y was derived through a similar procedure to that used to calculate the stiffness in the x direction. We changed the bias voltage and measured the resonant frequency for each bias voltage as shown in below.

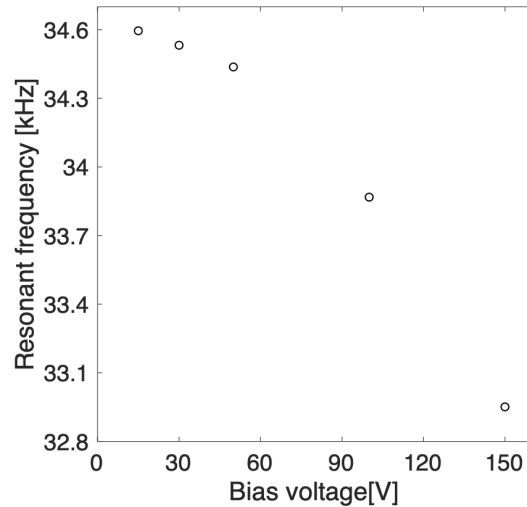


Figure S21 | The resonant frequencies of k_y beam were measure for each bias voltage. The resonant frequency at the bias voltage as 0 V corresponds to the stiffness of the beam.

According to the relationship between the bias voltage V_{bias} and the resonant frequency f , we obtained $f = -0.0742V_{bias}^2 + 0.0721V_{bias} + 34608$. We found that the resonant frequency for detecting the force was 34.608 kHz, because the resonant frequency when the bias voltage V_{bias} was zero, corresponds to the stiffness that does not include the spring effect. Therefore, we found that the stiffness k_y was 30 N/m.

$$k_y = 9.08 \times (34608)^2 \times 2329 \text{ [Kg/m}^3\text{]} \times (17.5 \times 10^{-6}) \times (850 \times 10^{-6}) \times (80 \times 10^{-6})$$

$$= 30.141 \text{ [N/m]}$$

$$= 30 \text{ [N/m]}$$

The stiffness of the beam agrees to within 1.4% via analytical, numerical and experimental means.

Supplementary Discussion 2 (the calculation to estimate the e-beam damage on the specimen)

The effect of the TEM electron beam was evaluated and shown to be negligibly small.

Displacement energy: When the energy E_e as described in below equation exceeds a specific threshold energy E_d , the electron beam can displace atomic nuclei to interstitial positions [1].

$$E_e = E_0(1.02 + E_0/10^6)/(465.7A)$$

Where the incident-electron energy E_0 of our TEM was 200 keV, and atomic weight A of Silver was 107.9. The energy E_e from the electron beam is calculated as 4.86 eV. The threshold energy E_d of silver is 25 eV [2,3] and it is 5 times higher than the energy due to the electron beam of TEM. Therefore, it cannot displace atomic nuclei to interstitial positions and thereby the beam does not degrade the crystalline perfection of the silver part. We concluded that the experimental aberrations due to the displacement energy can be considered negligible.

The current flowing on the surface of the specimen j_{sample} was calculated as below. We estimated the current flowing on the surface of the tip when the electron beam illuminates the specimen. The current density j_{all} , when the beam was enlarged up to 11 cm in diameter, was experimentally measured. This density was found to be

$$j_{all} = 0.5 \times 10^{-11} \quad [\text{A}/\text{cm}^2]$$

The current density j' , when the beam was narrowed down to 4cm in diameter, was calculated as below

$$\begin{aligned} j' &= j_{all} \{ \pi (11/2)^2 \} / \{ \pi (4/2)^2 \} \\ &= 4.5 \times 10^{-11} \quad [\text{A}/\text{cm}^2] \end{aligned}$$

The current density j_{sample} , which was applied to the specimen, was calculated as below.

$$\begin{aligned}
 j_{sample} &= j' (3\text{nm} \times 1000,000)^2 \\
 &= 4.05 \times 10^{-12} [\text{A}] \\
 &= 4.05 \quad [\text{pA}]
 \end{aligned}$$

Therefore, we calculated the current flowing on the 3nm square specimen at 1,000,000X magnification as 4.05 pA and found the surface current was negligibly small. Furthermore, since both tips are connected to GND, no charge accumulation occurs within the sample specimen.

The increase in the temperature ΔT due to the e-beam was calculated as below. According to the reference [4],

$$H = Q' J \quad (Q' = \rho Q)$$

$$Q = Q_c + Q_r$$

$$k \nabla^2 T = H$$

where, H is the energy transfer rate, Q is the average energy loss of an electron per unit length, J is the electron current density which is experimental obtained as $4.5 \times 10^{-11} [\text{A cm}^{-2}]$, Q_c is the Collision stopping power, $1.671 [\text{MeV cm}^2 \text{ g}^{-1}]$, Q_r is the radiative stopping power, $0.03201 [\text{MeV cm}^2 \text{ g}^{-1}]$, ρ is the mass density of silver, $10500 [\text{Kg m}^{-3}]$, k is the thermal conductivity of silver $420 [\text{W m}^{-1} \text{ K}^{-1}]$, the values of Q_c , Q_r for Ag were obtained by reference [5]. And then

$$\begin{aligned}
 H &= Q J \\
 &= (1.671 + 0.03201) \times 10500 \times 4.5 \times 10^{-11} [\text{MeV cm}^2 \text{ g}^{-1} \text{ Kg m}^{-3} \text{ A}^{-1} \text{ A cm}^{-2}] \\
 &= 8.037 \times 10^{-4} \quad [\text{eV cm}^{-3}]
 \end{aligned}$$

$$=1.286 \times 10^{-22} \quad [\text{J cm}^{-3}]$$

$$\nabla^2 T = (1.286 \times 10^{-22}) / (4.2) \quad [\text{J cm}^{-3}] / [\text{J s}^{-1} \text{ cm}^{-1} \text{ K}^{-1}]$$
$$= 3.062 \times 10^{-7} \quad [\text{K s nm}^{-2}]$$

The increase in the temperature, ΔT , when we shine the electron beam on the 1nm square specimen for one minute is therefore

$$\Delta T = 3.062 \times 10^{-7} \times 60$$

$$= 18 \quad [\mu\text{K}]$$

As such the heating rate is approximately one milikelvin per hour of observation, and therefore the increase in temperature due to the electron beam is negligibly small.

Supplementary Discussion 3 (the uncertainty analysis)

The values of the error were calculated as follows. We performed similar experiments for six trials. One of the trials was described in the main manuscript. The other five experiments were described in the Supplementary data. In this section, error value is discussed.

The error in sliding distance in the lateral axis Δx depends on the clarity of TEM images because the sliding distance of the tip was measured by marking a characteristic feature on the tip and tracking the feature. Although the TEM resolution is 0.1 nm, the outline of the tip has a slightly larger width, and it is impossible to precisely measure the displacement less than the thickness of the outline. The width of the outline depends on the magnification of TEM images and the values were found to be 0.2 nm.

$$\Delta x = 0.2 \text{ [nm]} \quad (11)$$

The friction force ΔF error was derived by the propagation of the error of the stiffness Δk_x and the error of the sliding distance Δx , because the force was calculated as the product of the rigidity of spring constant k and the displacement of the tip x .

$$\Delta F = \sqrt{\left(\frac{dF}{dk_x} \Delta k_x\right)^2 + \left(\frac{dF}{dx} \Delta x\right)^2} \quad (12)$$

$$\frac{dF}{dk_x} = x \quad (\because F = k_x x) \quad (13)$$

k_x was obtained by the measurement of the resonant frequency. It is possible to precisely read the peak of the resonant frequency with 10 Hz(Δf) accuracy. Therefore, the error of the stiffness Δk_x is as below.

$$\Delta k_x = \left(\frac{dk_x}{df_x} \right) \Delta f$$

$$\therefore \Delta k_x = \left(\frac{23}{200} \right) \frac{M f_x \Delta f}{\pi^2} \quad (\because f_x = 2\pi \sqrt{\frac{k_x}{0.23M}}) \quad (14)$$

(13), (14) give that

$$\frac{dF}{dk_x} \Delta k_x = x \left(\frac{23}{200} \right) \frac{M f_x \Delta f}{\pi^2} \quad (15)$$

$$\frac{dF}{dx} = k_x \quad (\because F = k_x x) \quad (16)$$

(16) gives that

$$\frac{dF}{dx} \Delta x = k_x \Delta x \quad (17)$$

Substituting (15) and (17) to (12),

$$\begin{aligned} \Delta F &= \sqrt{\{x \left(\frac{23}{200} \right) \frac{M f_x \Delta f}{\pi^2}\}^2 + (k_x \Delta x)^2} \\ &= 0.6 \text{ (nN)} \end{aligned} \quad (18)$$

Therefore the friction force error ΔF was derived as 0.6 nN. The displacement of the beam x is 3.8×10^{-9} m, the mass of the beam M is 8.0×10^{-10} Kg, the resonant frequency (experimental data) f_x is 6470 Hz, the error of the measurement Δf is 10 Hz, the stiffness of the beam k_x is 3.1 N/m, the error of the displacement Δx is the results of Eq.11.

The load error ΔL was derived through a similar procedure to that used to measure the error ΔF .

$$\begin{aligned} \Delta L &= \sqrt{\left(\frac{dL}{dk_y} \Delta k_y \right)^2 + \left(\frac{dL}{dy} \Delta y \right)^2} \\ &= \sqrt{\{y \left(\frac{23}{200} \right) \frac{M f_y \Delta f}{\pi^2}\}^2 + (k_y \Delta y)^2} \\ &= 6 \text{ (nN)} \end{aligned} \quad (19)$$

Therefore the friction force error ΔL was derived as 6 nN. The displacement of the beam x is 3.8×10^{-9} m, the mass of the beam M is 25.8×10^{-10} kg, the resonant frequency (experimental data) f_x is 10944 Hz, the error of the measurement Δf is 10 Hz, the stiffness of the beam k_x is 30 N/m, the error of the displacement Δx is the results of Eq.11.

The error of the shear force ΔF_{shear} was calculated as below. The shear force F_{shear} and the compressive force F_{normal} were obtained by Eq.20 where F is friction force, L is load, and θ is the angle between the direction of actuation and the plane of contact.

$$\begin{pmatrix} F_{shear} \\ F_{normal} \end{pmatrix} = \begin{pmatrix} \cos\theta & -\sin\theta \\ \sin\theta & \cos\theta \end{pmatrix} \begin{pmatrix} F \\ L \end{pmatrix} \quad (20)$$

Therefore the shear force error ΔF_{shear} was

$$\begin{aligned} \Delta F_{shear} &= \sqrt{\left(\frac{dF_{shear}}{dF}\Delta F\right)^2 + \left(\frac{dF_{shear}}{dL}\Delta L\right)^2 + \left(\frac{dF_{shear}}{d\theta}\Delta\theta\right)^2} \\ &= \sqrt{(\Delta F \cos\theta)^2 + (\Delta L \sin\theta)^2 + (\Delta\theta)^2 (F \sin\theta + L \cos\theta)^2} \\ &= \sqrt{(0.6 \times \cos 14.4)^2 + (6.0 \times \sin 14.4)^2 + (0.052)^2 (11.82 \times \sin 14.4 + 18.19 \times \cos 14.4)^2} \\ &= 1.93 \text{ (nN)} \end{aligned}$$

Therefore the error of friction force ΔF_{shear} was calculated to be 1.93 nN. The of friction force error ΔF is 0.6 nN, the friction force error ΔL is 6.0 nN, the value of the contact angle just prior to the separation θ : 14.4° , the value of friction force just prior to the separation F is 11.82 nN, the value of normal force just prior to the separation L is -18.19 nN, the contact angle error just prior to the separation $\Delta\theta$ is 4.0° .

The normal force error ΔF_{normal} was derived through a similar procedure to that used to measure the error ΔF_{shear} .

$$\begin{aligned}
\Delta F_{normal} &= \sqrt{\left(\frac{dF_{normal}}{dF} \Delta F\right)^2 + \left(\frac{dF_{normal}}{dN} \Delta N\right)^2 + \left(\frac{dF_{normal}}{d\theta} \Delta \theta\right)^2} \\
&= \sqrt{(\Delta F \sin \theta)^2 + (\Delta L \cos \theta)^2 + (\Delta \theta)^2 (F \cos \theta - L \sin \theta)^2} \\
&= 5.83 \text{ (nN)}
\end{aligned}$$

Therefore, the friction force error ΔF_{normal} was derived as 5.83 nN. Where the friction force error ΔF is 0.6 nN, the friction force error ΔN is 6.0 nN, the value of the contact angle just prior to the separation θ is 14.4° , the value of friction force just prior to the separation F is 11.82 nN, the value of normal force just prior to the separation N is 18.19 nN, the error of contact angle error just prior to the separation $\Delta\theta$ is 4.0° .

The value of the contact width w was measured by detecting both side of the junction. Therefore, the resolution Δx ($= \Delta y$) affects the contact width of the junction error Δw .

$$\begin{aligned}
\Delta w &= \sqrt{(\Delta x)^2 + (\Delta x)^2} \\
&= \sqrt{(0.3)^2 + (0.3)^2} \\
&= 0.29 \text{ [nm]}
\end{aligned}$$

The value of the von Mises stress S_{vM} was calculate by Eq.21. F_{shear} was shear force calculate by Eq.22. F_{normal} was the normal force calculate by Eq.23. and A was the actual contact area calculate by Eq.24 where w was the value of contact width.

$$S_{vM} = \sqrt{\sigma^2 + 3\tau^2} \quad (21)$$

$$\tau = \frac{F_{shear}}{A} \quad (22)$$

$$\sigma = \frac{F_{normal}}{w} \quad (23)$$

$$A = \pi \left(\frac{w}{2}\right)^2 \quad (24)$$

Therefore the von Mises stress error ΔS_{vM} was calculate by Eq.25.

$$\begin{aligned}
\Delta S_{vM} &= \sqrt{\left(\frac{dS_{vM}}{d\sigma}\Delta\sigma\right)^2 + \left(\frac{dS_{vM}}{d\tau}\Delta\tau\right)^2} \\
&= \sqrt{\left(\frac{\sigma^2}{\sigma^2 + 3\tau^2}\Delta\sigma^2\right) + \left(\frac{9\tau^2}{\sigma^2 + 3\tau^2}\Delta\tau^2\right)} \\
(\because \frac{dS_{vM}}{d\sigma} &= \frac{\sigma}{\sqrt{\sigma^2 + 3\tau^2}}, \frac{dS_{vM}}{d\tau} = \frac{3\tau}{\sqrt{\sigma^2 + 3\tau^2}}) \quad (25)
\end{aligned}$$

According to Eq.23,

$$\begin{aligned}
\Delta\sigma &= \sqrt{\left(\frac{d\sigma}{dF_{normal}}\Delta F_{normal}\right)^2 + \left(\frac{d\sigma}{dA}\Delta A\right)^2} \\
&= \sqrt{\left(\frac{\Delta F_{normal}}{A}\right)^2 + \left(\frac{F_{normal}}{A^2}\Delta A\right)^2} \quad (\because \frac{d\sigma}{dF_{normal}} = \frac{1}{A}, \frac{d\sigma}{dA} = \frac{-F_{normal}}{A^2}) \\
(26)
\end{aligned}$$

According to Eq.22,

$$\begin{aligned}
\Delta\tau &= \sqrt{\left(\frac{d\tau}{dF_{shear}}\Delta F_{shear}\right)^2 + \left(\frac{d\tau}{dA}\Delta A\right)^2} \\
&= \sqrt{\left(\frac{\Delta F_{shear}}{A}\right)^2 + \left(\frac{F_{shear}}{A^2}\Delta A\right)^2} \quad (\because \frac{d\tau}{dF_{shear}} = \frac{1}{A}, \frac{d\tau}{dA} = \frac{-F_{shear}}{A^2}) \quad (27)
\end{aligned}$$

According to (14), the actual contact area error is

$$\begin{aligned}
\Delta A &= \frac{dA}{dw}\Delta w \\
&= \frac{\pi}{2}w\Delta w \\
&= 2.15 \text{ [nm]} \quad (28)
\end{aligned}$$

Substituting (26), (27), (28) to (25),

$$\Delta S_{vM} = 0.29 \text{ [GPa]}$$

where the shear force error ΔF_{shear} is 1.93 nN, the value of shear force F_{shear} is 6.94 nN, the normal force error ΔF_{normal} is 5.83 nN, the value of normal force F_{normal} is -20.6 nN, the value of actual contact area just prior to the separation A is 11.8 nm², the value of shear stress just prior to the separation: 0.38 GPa, the value of normal stress just prior to the separation is -1.11 GPa, the contact width just prior to the separation w is 0.29 nm. The uncertainty values of all experiments were derived from similar procedures above.

Supplementary Discussion 4 (The calculation of the critical contact width)

Aghababaei et al. (17) calculated a critical contact width for this process to occur in shearing asperities based on the increase in the surface energy produced by fracture and the work done by external forces due to shear stress. If the contact width is smaller than the critical contact width, asperity fracture and wear debris is occurs. The critical contact width d^* is derived from Eq(1).

$$d^* = \frac{G\Delta w}{\sigma^2} \quad (1)$$

where Δw is the work adhesion of silver as 2.516(J/m²), G is the shear modulus as 27.8(GPa), σ is the shear stress at separation. The experimental data of shear stress at separation are 0.38, 0.36, 0.41, 0.37, 0.10, and 0.14(GPa). Thus each value of the critical contact width is 1476, 1628, 1242, 1549, 20168, and 10705(nm). And the contact width obtained from TEM images are 5.46, 4.56, 7.21, 7.12, 10.69, and 8.96 respectively. It was found that the critical contact widths were 170-1900 times larger than the values of the contact width obtained from the experiments. Thus, the model of Aghababaei et al. predicts no asperity fracture, consistent with our results.

Reference

- [1] R. F. Egerton, P. Li and M. Malac "Radiation damage in the TEM and SEM" micron, 35, 399-409, 2004
- [2] Hobbs, L. W., 1987. Radiation effects in analysis by TEM. In: Hren, J. J., Goldstein, J. I., Joy, D. C. (Eds.), Introduction to Analytical Electron Microscopy, Plenum Press, New York, pp. 399–445.
- [3] A. Yu. Konobeyev, U. Fischer, Yu. A. Korovin, S. P. Simakov "Evaluation of effective threshold displacement energies and other data required for the calculation of advanced atomic displacement cross-sections" Nuclear Energy and Technology, 3, 169-175, 2017
- [4] Kun Zheng, Chengcai Wang, Yong - Qiang Cheng, Yonghai Yue, Xiaodong Han, Ze Zhang, Zhiwei Shan, Scott X Mao, Miaomiao Ye, Yadong Yin and Evan Ma "Electron-beam-assisted superplastic shaping of nanoscale amorphous silica" Nature Communications, 2010, vol.1, p.24
- [5] Berger, M. J., J. H. Hubbell, S. M. Seltzer, J. Chang, J. S. Coursey, R. Sukumar, and D. S. Zucker. "NIST standard reference database." (2010)